International Journal of
Geohazards and Environment
http://ijge.camdemia.ca, ijge@camdemia.ca
IJGE 2016 2(4): 208-213
Available at http://ojs.library.dal.ca/ijge

Prediction of Magnitude and Epicentral Distance from a Single Seismic Record: A Case Study of the Ahar-Varzaghan Earthquake

Majid Mahood*, Mohammad Mokhtari, Hamid Zafarani
Earthquake Prediction Center, International Institute of Earthquake Engineering and Seismology, Tehran, Iran

Abstract: Earthquake magnitude and P wave amplitude (P_{max}) are important parameters for Earthquake Early Warning Systems (EEWS), yet their dependence on source mechanism, focal depth and epicentral distance (Δ) has not been fully studied. We examined a method to estimate an earthquake's magnitude and epicentral distance using the initial part of P-wave data (within 3 s) for application in EEWS. The *B-Δ* method is used to estimate the epicentral distance from a single station data in a short time. Fitting a simple function with the form of $y(t) = Bt \times exp(-At)$ to the first few seconds of the waveform envelope, coefficients A and B are determined through the least-squares method. $LogB$ is inversely proportional to $log\Delta$, where Δ is the epicentral distance. This relation holds true regardless of earthquake magnitude. B values are calculated on the basis of 48 vertical-component accelerograms of the Ahar-Varzaghan earthquake in a magnitude range Mw4.5-6.4 and epicentral distances less than 100 km. Using this method, we could estimate the epicentral distance by $log\Delta = -0.69\ logB + 2.5$ and earthquake magnitude by $M_{est} = 1.89\ logP_{max} - 1.76\ logB + 5.52$. The greatest advantage of this method is its accuracy and rapidness.

Keywords: Earthquake Early Warning Systems, B-Δ method, Single Station records, Ahar-Varzaghan Earthquake, Northwestern Iran

1 Introduction

Magnitudes and locations are the two first-order important features for earthquakes recorded during seismic activities. Magnitude indicates the strength of an event and may also reveal the fracturing processes and the fault geometry. Although magnitude may seem straight forward to calculate, a number of different magnitude scales have been proposed over the years. Most of these scales are empirical and do not relate magnitude to a physical model. An exception is the moment magnitude, introduced by Hanks and Kanamori (1979), which can be used to bridge waveform amplitudes to seismic moment, involving rock rigidity, fault area and seismic slip. Odaka et al (2003) presented a novel method of estimating the magnitude and epicentral distance from a single seismic record in a short amount of time, say, a few seconds after the P-wave arrival. This method is called *B-Δ* method. They have found that the envelope waveform of the initial part of a P-wave changes systematically with magnitude and epicentral distance. Using this method, the Shinkansen Earthquake Early Warning System (EEWS) in Japan rapidly estimates earthquake parameters from a single station data (Noda et al 2012).

One of the systems that is now under practical use, called Urgent Earthquake Detection and Alarm System (UrEDAS) (Bito and Nakamura 1986, Nakamura 1988), which has been used by railways network to stop trains during an earthquake occurrence in Japan. In the UrEDAS system, the magnitude is determined on the basis of the predominant period of P waves, which may become longer with increasing magnitude. The pilot TDMMO (Tehran Disaster Mitigation and Management Organization) warning system is in its final stage for running experimental tests. The *B-Δ* algorithm has been used and the relation developed by Japan Meteorological Agency (JMA) is used for rapid estimation of magnitude and epicentral distance (Heidari 2016). Istanbul Earthquake Early Warning and Rapid Response System (IEEWRRS) has been deployed in 2002. In 2012, Istanbul Natural Gas Distribution Company (IGDAS) has started a project of IGDAS Earthquake Risk Reduction System collaboration with KOERI, Turkey. The main aim was to establish a real-time risk reduction system for the whole natural gas network (Zulfikar et al 2014).

In this study, distance and magnitude are investigated from a single-station record of the Ahar-Varzaghan earthquakes in NW Iran. Magnitude estimation is then readily performed on the basis of the P-wave maximum amplitude within a given short time interval after the P-wave arrival.

2 Study Region

The region of NW Iran is exceptional within the Arabian-Eurasian continental collision zone. The tectonics is

* Corresponding Author: Majid Mahood, Email: m.mahood@iiees.ac.ir, Tel: +98 (21) 2283-1116

DOI: 10.15273/ijge.2016.04.019

dominated by the NW-SE striking right-lateral North Tabriz Fault (NTF), which is a major seismogenic fault in this region. Historical seismicity in the northwest of Iran is mostly associated with this Fault (Figure 1). Figure 1 presents an overview of northwestern Iran with topography, position of the Ahar-Varzaghan earthquake sequence, broadband stations and major faults as well as focal mechanisms for both largest main shocks according to different international agencies. The last major damaging earthquakes on the NTF one occurred in 1721, rupturing the southeastern fault segment, and another in 1780, rupturing the northwestern part. Understanding of the seismic behaviour of this fault is critical for assessing the hazard in Tabriz, one of the major cities in Iran; the city suffered major damage in both the 1721 and 1780 events. North of the NTF seismicity is rare.

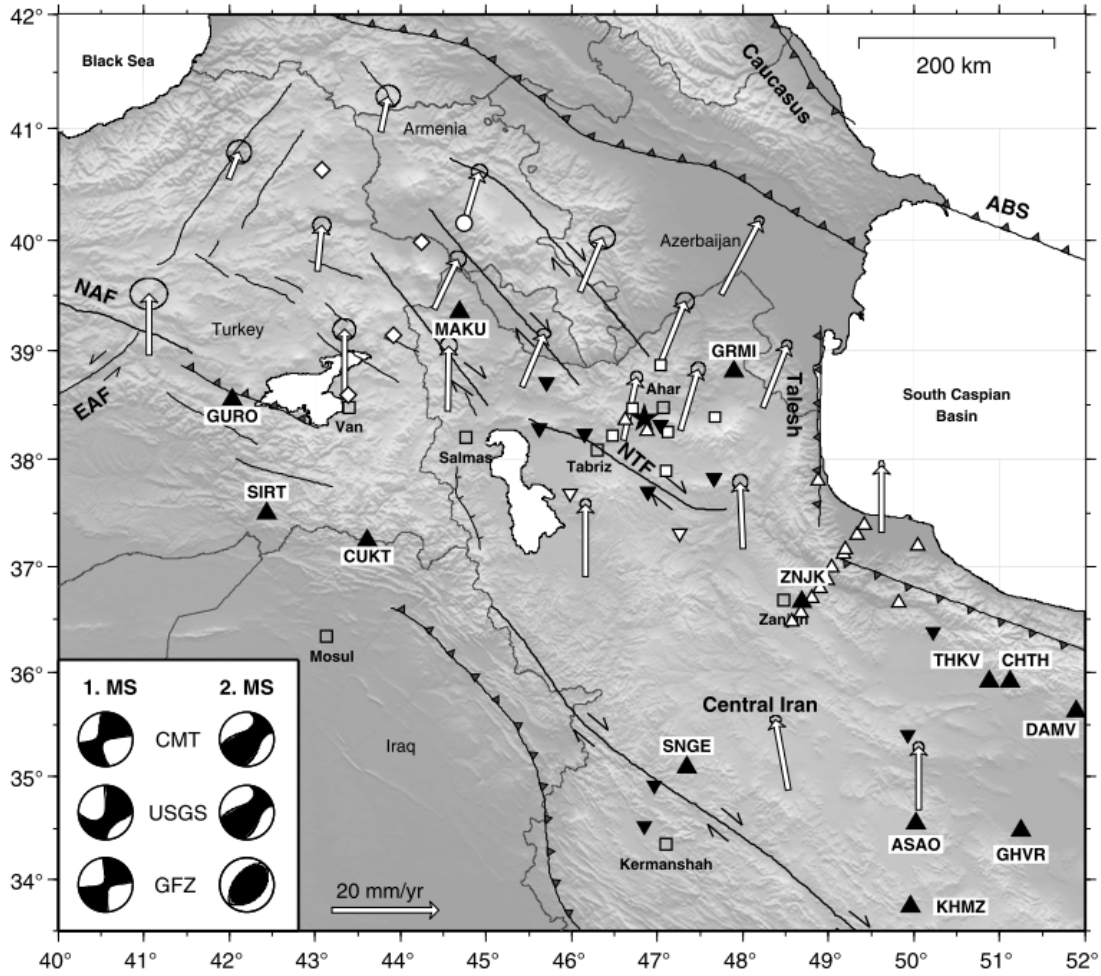

Figure 1. Overview of seismicity of NW Iran (Donner et al 2015). The star marks the position of the Ahar-Varzaghan earthquake. NTF – North Tabriz fault; NAF – North Anatolian fault; EAF – East Anatolian fault. Arrows give Global Positioning System velocities and 95% confidence ellipses relative to Eurasia selected from Djamour et al (2011). Black triangles – broadband stations of the Iranian National Seismic Network and the Turkish National Broadband Network. Black inverted triangles – short-period stations of the Iranian Seismic Telemetry Network. Reversed triangles – Iranian Seismological Center (IRSC); diamonds – Kandilli Observatory and Earthquake Research Institute (KOERI); circle – Incorporated Research Institutions for Seismology (IRIS); rectangles – Building and Housing Research Center (BHRC). Inset shows the mechanisms for both main shocks according to international agencies: Global Centroid Moment Tensor Project (Global CMT), U.S. Geological Survey (USGS), GEOFON Global Seismic Network (GFZ).

On August 11, 2012, the region was surprisingly struck by a shallow Mw6.4 earthquake with pure right-lateral strike-slip character only about 50 km north of the NTF. It produced an east–west oriented surface rupture of about 12 km length (Faridi and Sartibi 2012). Only 11 minutes later, a second event with Mw6.2 occurred in about 6 km further NW (Ghods et al 2015, Zafarani et al 2015). It showed an NE-SW oriented oblique thrust mechanism. The Ahar-Varzaghan doublet occurred in a region that has been characterized as having a low deformation rate and being bounded by deep-seated faults, among which the NTF is the most important (Hessami et al 2003, Ghods et al 2015, Donner et al 2015). Such a characterization is consistent with the seismic record, until 2012. This earthquake sequence provides an opportunity to better understand the processes of active deformation and their causes in NW Iran.

3 Estimation of Magnitude and Epicentral Distance

Envelope of seismic waves can differ depending on earthquake magnitude, focal depth, and epicentral distance; ground motion can be displayed on a logarithmic scale to determine these differences visually (Odaka et al 2003). The noise levels (the small-amplitude initial portion of the P-phase) preceding the arrival of P-wave, and the large amplitude later phases (i.e. the S-phase) can then be recognized easily and the differences in waveform characteristics immediately understood (Figure 2). Logarithmic waveforms have shown that the initial parts of seismic waves (within several seconds after P-wave arrival) vary systematically in response to earthquake magnitude and epicentral distance. The following function can be used to quantitatively evaluate differences in waveform:

$$y(t) = Bt \times exp(-At) \quad (1)$$

where, $y(t)$ is the waveform envelope constructed from observed seismic waveform $x(t)$, the origin time t is taken at P-wave arrival time. First, a nonnegative waveform is constructed by taking absolute values of the original waveform $x(t)$. Second, the waveform envelope $y(t)$ is constructed. Figure 2 shows an example which the envelope was simply constructed by taking the maximum amplitude (e.g. for a 0.1 s time window). The unknown parameters A and B are determined using the least-squares method (Figure 2). Using a fitting curve in the form of $Bt \times exp(-At)$ has the effect of applying low-pass filtering (smoothing) to waveform data. This method is not affected by contamination due to high-frequency noise (Odaka et al 2003, Noda et al 2012). The parameter B defines the slope of the initial parts of the P-waves, and A is related to amplitude variation over time.

Figure 2(a) shows a vertical-component accelerogram recorded from the first Ahar-Varzaghan earthquake (Mw6.2) and (b) detection of the P-wave. P-wave start time should be measured very accurately to avoid any mistakes in evaluation of A and B values. Also, Figure 2(c) shows logarithm of absolute values for the selected waveform with epicentral distance of 24 km in the NW-Iran (Rec. No. 5520-1). The continuous line on Figure 2(c) indicates the fitting of function $Bt \times exp(-At)$ to an envelope of amplitudes. The initial low-amplitude part of seismogram denotes the noise and the slope rising sharply from the noise level indicates the P-wave arrival.

Figure 3 shows the relationship between epicentral distance and the coefficient B. B values are calculated on the basis of 48 vertical-component accelerograms of the Ahar-Varzaghan earthquake sequence with magnitude range Mw4.5-6.2, recorded by the BHRC (Building and Housing Research Center). The data length used in the analysis was 3 s after the start of P-wave. It is clear from Figure 3 that $LogB$ is linearly proportional to $-Log\Delta$, where Δ denotes the epicentral distance. Note that this relation seems to be independent of earthquake magnitude (Odaka et al 2003). The dispersion of data is not large and this result is important because a regression line can be obtained via the least-

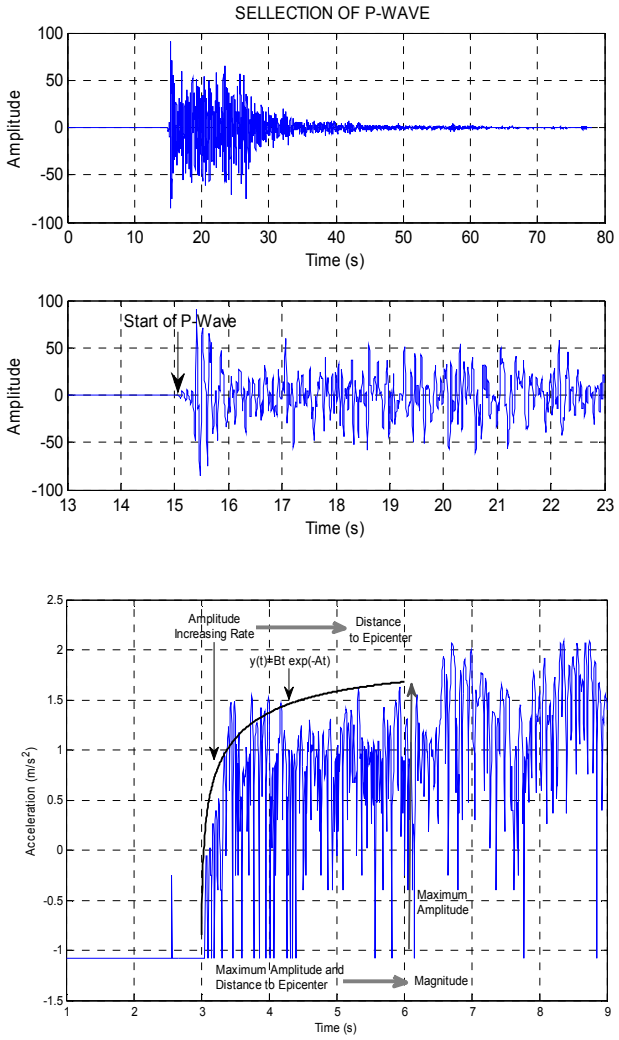

Figure 2. (a) Vertical-component accelerogram recorded Mw6.2, (b) detection of the P-wave, and (c) logarithm of absolute values for the Selected waveform. The continuous line indicates the fitting of function $Bt \times exp(-At)$ to an envelope of amplitudes.

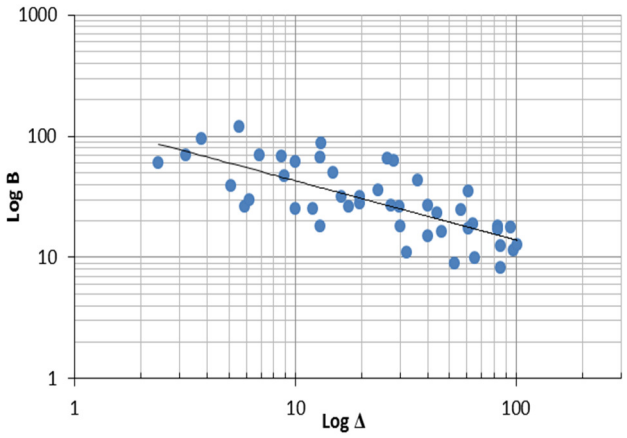

Figure 3. Relationship between coefficient B (initial slope of envelope of P-waves) and epicentral distance Δ.

square method, as a relation between $logB$ and $log\Delta$, and this regression line can be used to estimate an epicentral distance from the value of B. The azimuth of the epicentre, as seen from an observation station, can be inferred from the ratio of two horizontal-component P-wave first motions and the polarity of a vertical-component P-wave motion (Odaka et al 2003, Noda et al 2012). The location of the epicentre can then be estimated by P-wave recognition and epicentral azimuth estimation using three components of the single station.

As mentioned, the epicentral distance can be estimated immediately after the arrival of P-wave by determining the empirical relationship between the coefficient B and epicentral distance. If early earthquake warnings are to be effective, earthquake size must be evaluated quickly. Earthquake magnitude could be estimated using the following formula (Odaka et al 2003):

$$M_{est} = a\ logP_{max} - b\ logB + c \qquad (2)$$

where, M_{est} represents the estimated magnitude and P_{max} the maximum amplitude of P-wave within any specified short time interval (e.g., 3 s) after the arrival of P-wave. The constants a, b, and c can be determined empirically.

4 Results and Discussion

With the abovementioned method, the time required for estimating the distance to the epicentre is quite short. In the present study, there is a good linear relationship between $logB$ and $log\Delta$, as can be seen in Figure 3. The relation for the 3 s time window for the Ahar-Varzaghan region, NW-Iran is as follows:

$$log\Delta = -0.69\ logB + 2.5 \pm 0.4 \qquad (3)$$

Earthquake magnitude is obtained as a function of maximum phase amplitude received during the initial seconds and epicentral distance. In this study, earthquake magnitude is estimated by the following formula:

$$M_{est}=1.89\ logP_{max} - 1.76\ logB + 5.52 \pm 0.36 \qquad (4)$$

In Figure 4, we show an example of waveforms varying with epicentral distance. Graphs are for two stations in distances of 107 km and 18 km, respectively, to the Ahar-Varzaghan earthquake center. The initial low-amplitude part of each seismogram denotes the noise and the slope rising sharply or gradually from the noise level indicates the P-wave arrival. Comparison of the two graphs shows that the rising envelop slope becomes gentle with increasing epicentral distance. The slop of waveform envelop in 18 km is sharper than the other.

Odaka et al (2003) described the amplitude of the large earthquake increases gradually with time, whereas that of the small earthquake decreases soon after P-wave arrival, which is consistent with the observation by other researchers (Noda et al 2012). Figure 5 shows a near field record where S-waves arrive in time of less than 3 s. It may be impossible to

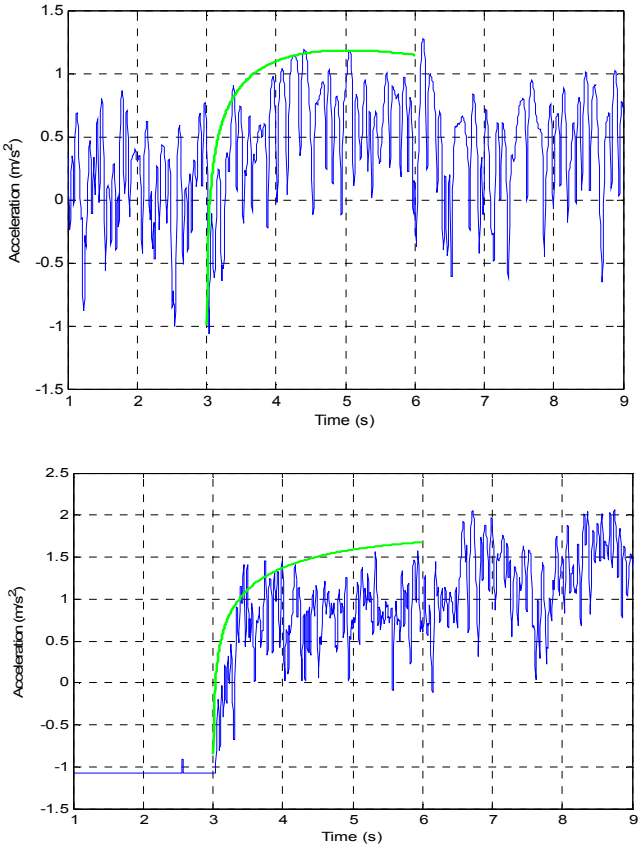

Figure 4. Comparison between two waveforms that vary in form with epicentral distance of the Ahar-Varzaghan earthquake Mw6.2. Light curves are the fitting curves of the form $Bt\times exp(-At)$

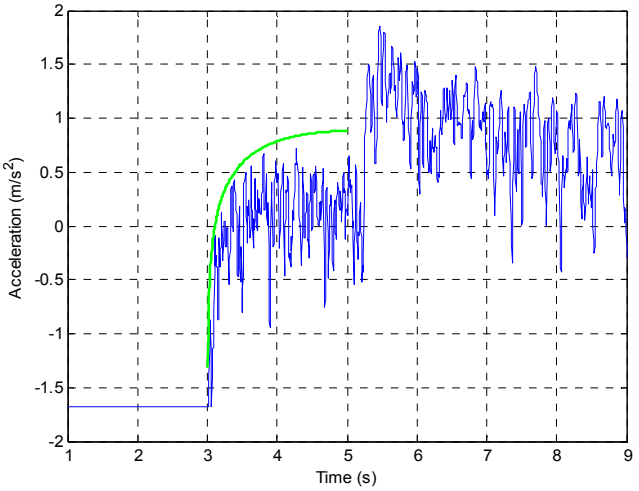

Figure 5. Vertical-component accelerogram recorded Mw5.2 and Δ = 15 km

estimate the magnitudes and distances of very local earthquakes in 3 s of initial part of P-wave. In this condition time window intervals can be set to 2 s and errors will increase.

We have compared the M_{est} and the observed (M_{obs}) values to test the reliability of the magnitude estimation (Figure 6, Top). It is clear that differences between predicted and observed values are almost insignificant. Furthermore, comparison between observed and estimated magnitudes with epicentral distance is shown in Figure 6. Estimated values for records with an epicentral distance more than 70 km are smaller than observed values. Attenuation of seismic wave in the active region of Iran (tectonically active zones characterized by a high degree of heterogeneity) is high and it can be the reason of underestimation of the magnitude (Mahood 2014).

It would be more appropriate to compare with other active regions in order to observe whether characteristics are present in the study area. As a result of tectonic differences in active regions, such linear relations have a different slope relative to the relation applied in other regions and consequently each active seismic region needs a specific relation. Figure 7 shows the comparison of this study with relationships developed for the Tehran region and Japan. The obtained relationship is generally similar to the relation developed for the Tehran region (Heidari 2016).

Noda et al (2012) obtained a new *B*-*Δ* relation and presented new methods to improve the performance of epicentre estimation by introducing variable time windows, instead of the conventional fixed time window for Japan. Odaka et al (2003), based on the results of their earlier numerical experiment, recommended 2 or 3 s for the time window. They mentioned that it might be difficult to estimate the magnitudes of large earthquakes (e.g., Mw8 earthquakes) within such a short time after P-wave arrival because the duration time of the rupture is far longer than 2 to 3 s. This problem is addressed by calculating magnitudes repeatedly with lapses of time and time window intervals can be set to 2 or 3 s, and so on. When amplitudes of P-waves increase with time, estimated magnitudes may also become large. Odaka et al (2003) expected that *A* parameter may be useful for distinguishing shallow and deep earthquakes, and large and small earthquakes. The greatest advantage of this method is its accuracy and rapidness, and it can be used for all faulting mechanisms.

5 Conclusion

This study used a practical method to improve performance in estimation of the magnitude and epicentral distance. This method can apply as a new stand-alone seismographic system that detects an earthquake and issues a warning immediately after the arrival of P-wave. The epicentral distance is estimated from the coefficient *B* which is determined by fitting the equation $y = Bt \times exp(-At)$ to the vertical component envelop of the accelerograms of the initial P-wave. Coefficient *B* is almost independent of

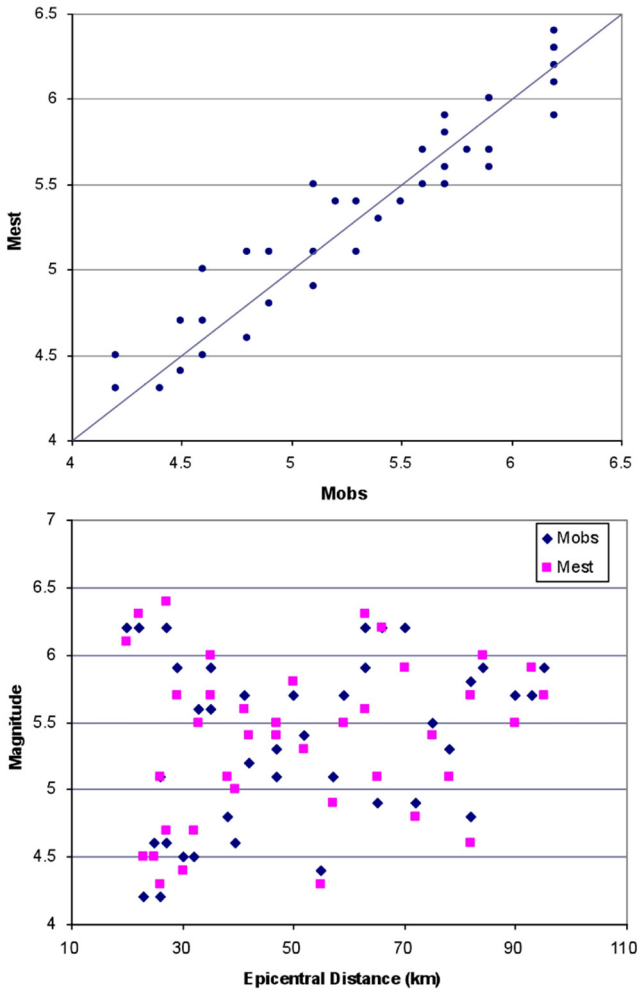

Figure 6. Top: Comparing values for M_{est} and M_{obs}. Bottom: Comparison between observed and estimated magnitudes with respect to epicentral distance

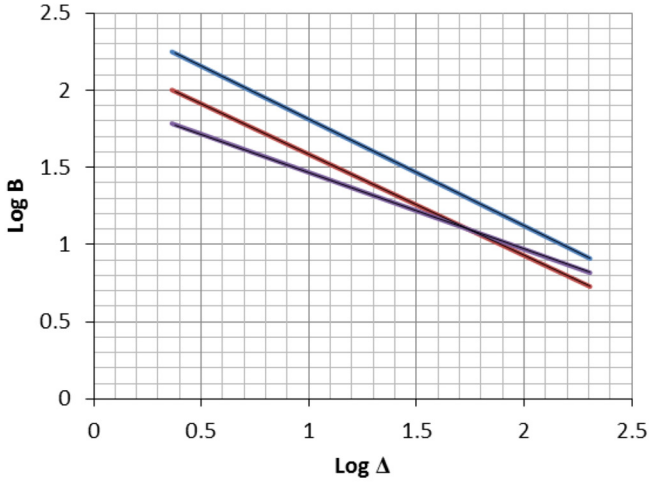

Figure 7. Comparison between different tectonic regions: this study, Tehran area (based on Heidari 2016) and Japan (based on Okada et al 2003)

magnitude, which is mainly affected by epicentral distance. Moreover, to develop magnitude-scaling relation for earthquakes, P_{max} within the initial 3 s of P-wave arrival is used. In the current study, earthquake magnitude is estimated using an empirical magnitude–amplitude relation that includes the epicentral distance as an input parameter.

Acknowledgements

The authors would like to express their thanks to reviewers for carefully commenting on the manuscript. The authors also want to acknowledge International Institute of Earthquake Engineering and Seismology (IIEES) for supporting this research (Project number 9618/662) and providing the data.

References

Bito, Y. and Y. Nakamura, 1986. Urgent earthquake detection and alarm system. In: Civil Engineering in Japan. Japan Society of Civil Engineers, Tokyo, 103 - 116.

Djamour, Y., P. Vernant, H.R. Nankali and F. Tavakoli, 2011. NW Iran eastern Turkey present-day kinematics: Results from the Iranian permanent GPS network. Earth Planet. Sci. Lett, **307**: 27 - 34.

Donner, S., A. Ghods, F. Krüger, D. Rößler, A. Landgraf and P. Ballato, 2015. The Ahar-Varzaghan Earthquake Doublet (Mw6.4 and 6.2) of 11 August 2012: Regional Seismic Moment Tensors. Bull Seismol Soc Am **105**(**2A**): 791 - 807.

Faridi, M. and A. Sartibi, 2012. Report of the Ahar Varzaghan earthquake on 11 August 2012. Technical Report, Geological Survey of Iran, p27.

Ghods, A., E. Shabanian, E. Bergman, M. Faridi, S. Donner, G. Mortezanejad and A. Aziz-Zanjani, 2015. The Varzaghan–Ahar, Iran, Earthquake Doublet (Mw6.4, 6.2): implications for the geodynamics of northwest Iran. Geophys. J. Int. **203**: 522 - 540.

Hanks, T.C. and H. Kanamori, 1979. A moment magnitude scale. J. Geophys. Res., **48**: 2348 - 2350.

Heidari, R., 2016. Quick Estimation of the magnitude and epicentral distance using P wave for earthquakes in Iran. Bull. Seismol. Soc. Am., **106**: 225-231.

Hessami, K., F. Jamali and H. Tabassi, 2003. Major Active Faults of Iran (map). Ministry of Science, Research and Technology, International Institute of Earthquake Engineering and Seismology.

Mahood, M., 2014. Attenuation of high-frequency seismic waves in Eastern Iran. Pure Appl. Geophys., **171**: 2225 - 2240.

Nakamura, Y., 1988. On the urgent earthquake detection and alarm system (UrEDAS). In: Proceedings of Ninth World Conference on Earthquake Engineering, Japan, Vol. VII: 673 - 678.

Noda, S., S. Yamamoto and S. Sato, 2012. New method for estimation earthquake parameters for earthquake early warning system. Railway Tech. Res. Inst., Tokyo, Quarterly Reports. **53**(**2**):

Odaka, T., K. Ashiya, S. Tsukada, S. Sato, K. Ohtake and D. Nozaka, 2003. A new method of quickly estimating epicentral distance and magnitude from a single seismic record. Bull. Seismol. Soc. Am., **93**: 526 - 532.

Zafarani, H., M. Rahimi, A. Noorzad, B. Hassani, B. Khazaei, 2015. Stochastic simulation of strongmotion records from the 2012 Ahar–Varzaghan Dual Earthquakes, Northwest of Iran. Bull. Seismol. Soc. Am., **105**:1419 - 1434.

Zulfikar, C., A. Pinar, E. Safak and M. Erdik, 2014. Implementation of EEWS to Istanbul Natural Gas Network. 3rd Int. Conference on Earthquake Early Warning, California.